

rate gives an expression for the proton-trapping lifetime that balances the CRAND source:

$$T_p = \frac{J_p}{J_n} T_n \quad (8)$$

At  $2.7 R_S$ , the proton flux above 80 MeV is  $\sim 2 \times 10^4 \text{ cm}^{-2} \text{ sec}^{-1}$  and the neutron lifetime is 13 minutes. It is possible to calculate the neutron albedo flux at Saturn, but such an effort is beyond the scope of this report. To test the reasonability of our speculation, we merely write  $J_n$  as some factor  $F$  times the albedo neutron flux at Earth. The latter is  $\sim 0.1 \text{ cm}^{-2} \text{ sec}^{-1}$  for neutrons above 80 MeV (24), so we obtain, for the proton trapping lifetime that balances the CRAND source,  $T = \sim 7.5/F$  years. If  $F$  is of the order of unity, this number is easily compatible with the diffusive loss time  $T_a$ . However, a more satisfying comparison must await a more extensive calculation.

W. FILLIUS

University of California, San Diego,  
La Jolla 92093

W. H. IP

Max-Planck-Institut für Aeronomie,  
Katlenburg-Lindau, West Germany

C. E. MCLWAIN

University of California, San Diego

#### References and Notes

1. B. A. Smith *et al.*, *Science* **204**, 951 (1979).
2. M. H. Acuña and N. F. Ness, *J. Geophys. Res.* **81**, 2917 (1976); W. Fillius, in *Jupiter*, T. Gehrels, Ed. (Univ. of Arizona Press, Tucson, 1976), pp. 896-927.
3. E. J. Smith, L. Davis, Jr., D. E. Jones, P. J. Coleman, Jr., D. S. Colburn, P. Dyal, C. P. Sonett, *Science* **207**, 407 (1980); M. H. Acuña and N. F. Ness, *ibid.*, p. 444.
4. All times given in this report are universal time at the spacecraft, which is obtained from ground-received universal time by deducting the one-way travel time of light (about 1 hour 26 minutes 20 seconds).
5. C. E. Mclwain, *J. Geophys. Res.* **66**, 3681 (1961).
6. In this report,  $L$  is the distance from the center of the planet to the equatorial crossing of the magnetic line of force through an observation point. It was computed by using a dipole field model with zero tilt and offset.
7. The unit of distance is the planetary radius,  $R_S$ , equal to 60,000 km.
8. J. H. Wolfe, J. D. Mihalov, H. R. Collard, D. D. McKibbin, L. A. Frank, D. S. Intriligator, *Science* **207**, 403 (1980).
9. J. W. Dyer, *ibid.*, p. 400.
10. E. C. Stone, *J. Geophys. Res.* **68**, 4157 (1963); J. G. Roederer, *Dynamics of Geomagnetically Trapped Radiation* (Springer-Verlag, New York, 1970).
11. J. H. Trainor, F. B. McDonald, A. W. Schardt, *Science* **207**, 421 (1980).
12. M. Schulz and L. J. Lanzerotti, *Particle Diffusion in the Radiation Belts* (Springer-Verlag, New York, 1974).
13. S. E. DeForest, *J. Geophys. Res.* **77**, 651 (1972).
14. T. Gehrels *et al.*, *Science* **207**, 434 (1980).
15. W. H. Blume *et al.*, in preparation.
16. R. W. Fillius and C. E. Mclwain, *J. Geophys. Res.* **79**, 3589 (1974); J. A. Simpson, D. C. Hamilton, R. B. McKibbin, A. Mogro-Campero, K. R. Pyle, A. J. Tuzzolino, *ibid.*, p. 3522.
17. J. A. Van Allen, M. F. Thomsen, B. A. Randall, R. L. Rairden, C. L. Grosskreutz, *Science* **207**, 415 (1980); J. A. Simpson *et al.* (20).
18. D. Morrison and D. P. Cruikshank, *Space Sci. Rev.* **15**, 641 (1974).

19. A. Mogro-Campero and W. Fillius, *J. Geophys. Res.* **81**, 1289 (1976).
20. J. A. Simpson, T. S. Bastian, D. L. Chenette, G. A. Lentz, R. B. McKibbin, K. R. Pyle, A. J. Tuzzolino, *Science* **207**, 411 (1980).
21. N. C. Christofilos, *J. Geophys. Res.* **64**, 869 (1959); P. B. Kellogg, *Nuovo Cimento* **11**, 48 (1959); S. F. Singer, *Phys. Rev. Lett.* **1**, 181 (1958); S. N. Vernov, special lecture to the Fifth General Assembly of the Comité Spécial de l'Année Géophysique Internationale, Moscow, 30 July to 9 August 1958.
22. F. Reif, *Fundamentals of Statistical and Thermal Physics* (McGraw-Hill, New York, 1974), pp. 486-488.
23. C. Kittell, *Elementary Statistical Physics* (Wiley, New York, 1958), p. 155.
24. R. E. Lingenfelter, in *Spallation Nuclear Reactions and Their Applications*, B. S. P. Shen and M. Merker, Eds. (Reidel, Dordrecht, Netherlands, 1976), pp. 193-205.

25. We are grateful to S. E. DeForest, E. Whipple, B. Johnson, J. Quinn, M. Greenspan, and C. Olson for assistance with the real-time data. C. Barnes, I. Goldman, and J. B. Blake made generous contributions to the detector calibrations, and E. Smith provided magnetometer data. Discussions with R. E. Lingenfelter were very helpful. The success of the Pioneer spacecraft reflects the superlative job done by the Pioneer Project Office under the leadership of C. F. Hall. This work was supported by NASA contract NAS 2-6552 and by NASA grant NGL-05-005-007.

3 December 1979

## Ultraviolet Photometer Observations of the Saturnian System

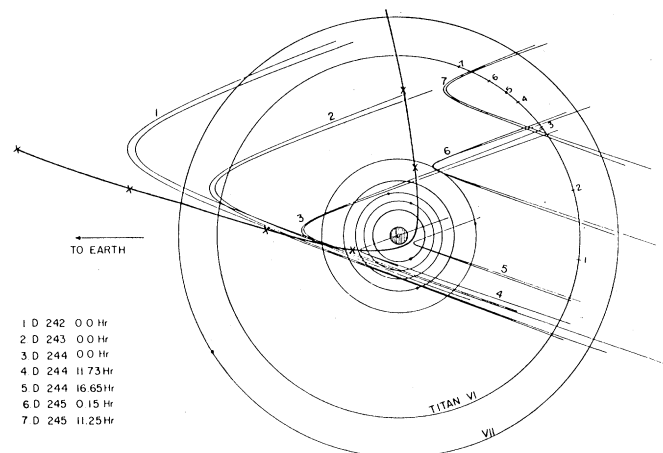
**Abstract.** Several interesting cloud and atmospheric features of the Saturn system have been observed by the long-wavelength channel of the two-channel ultraviolet photometer aboard the Pioneer Saturn spacecraft. Reported are observations of the most obvious features, including a Titan-associated cloud, a ring cloud, and the variation of atmospheric emission across Saturn's disk. The long-wavelength data for Titan suggest that a cloud of atomic hydrogen extends at least 5 Saturn radii along its orbit and about 1.5 Saturn radii vertically. A ring cloud, thought to be atomic hydrogen, has also been observed by the long-wavelength channel of the photometer; it shows significant enhancement in the vicinity of the B ring. Finally, spatially resolved observations of Saturn's disk show significant latitudinal variation. Possible explanations of the variation include aurora or limb brightening.

The ultraviolet photometer on Pioneer Saturn covers two broad spectral regions (1, 2). The short-wavelength ( $\lambda_S$ ) band is sensitive only to emissions shortward of about 800 Å and includes the 584-Å resonance line of helium. The region of sensitivity of the long-wavelength ( $\lambda_L$ ) channel includes the hydrogen resonance line at 1216 Å. The instrument design was based on the assumed dominance of hydrogen and helium gases in the Jupiter and Saturn systems. Accordingly, the emission signal in the  $\lambda_L$  channel is interpreted as resulting mainly from hydrogen emission at 1216 Å, while the signal in the  $\lambda_S$  channel is considered to be due to helium emission at 584 Å and perhaps

other species that emit shortward of  $\sim 800$  Å.

The field of view of the photometer is limited by a mechanical collimator whose optical axis is oriented at an angle  $\theta_0 = 20^\circ$  with respect to the spacecraft spin axis. The scanning motion that results from spacecraft rotation sweeps the field of view over the surface of a  $40^\circ$  cone whose vertex is on the spacecraft spin axis and whose axis of symmetry is oriented along the spin axis. The spin axis of the spacecraft is parallel to the spacecraft-Earth line. Figure 1 shows the trajectory of the spacecraft and the field of view of the photometer projected on the Saturn equatorial plane near the Sat-

Fig. 1. Viewing hyperbolas in Saturn's equatorial plane as seen from above Saturn's north pole. The width of the hyperbolas represents the  $1^\circ$  cone angle width over which the photometer is sensitive. The view in the plane of the satellite orbits corresponds to seven different spacecraft positions indicated by the seven hyperbolas. Titan is at position 1 when the photometer view is that indicated by hyperbola 1.



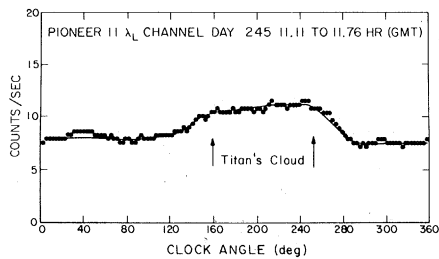
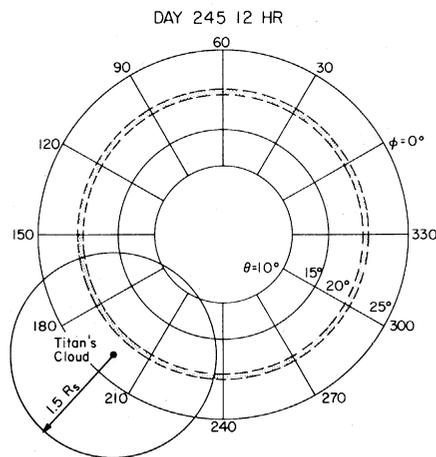


Fig. 2 (left). Emission signals detected by the  $\lambda_{L1}$  channel. The feature centered at clock angle  $\sim 210^\circ$  is interpreted as resonance scattering of the solar Ly  $\alpha$  line by atomic hydrogen in an extended region of space ( $\sim 1.5 R_S$ ) centered on Titan. Fig. 3 (right). Viewing geometry for the ultraviolet photometer at 1200 on day 245, as seen looking along the spin axis of the spacecraft. The dashed circle represents the field of view. The signal was observed to extend from  $160^\circ$  to  $240^\circ$  and indicates that the extent of Titan's cloud is  $\sim 1.5 R_S$  from Titan's center.



urn encounter. As the spacecraft approached Saturn, the photometer field of view swept through Titan's orbit, Saturn's rings, and across the planetary disk. The observed  $\lambda_{L1}$  signals from those objects throughout the encounter period are presented below. The data are presented as the observations were made, moving from the outermost feature, Titan, to the innermost feature, Saturn. In all cases, the observed emissions are assumed to be due to an atomic hydrogen Lyman  $\alpha$  (Ly  $\alpha$ ) glow in a tenuous atmosphere or cloud, consistent with the spectroscopic observation of Saturn and its ring system by Weiser *et al.* (3) and

Barker's identification of Ly  $\alpha$  from the vicinity of Titan (4).

**Titan observations.** Titan and its cloud were in the field of view during most of day 245. Emission signals were detected when Titan was in the center of the field of view ( $\theta = 20^\circ$ ) on day 245 at 1400 and 1530 Spacecraft Universal Time. However, the disk itself was not an obvious feature (Fig. 2). In addition, continuous emission signals were observed from 2300 on day 244 to 1330 on day 245, with the maximum emission occurring at about 1100 on day 245, when Titan's disk was about 2 Saturn radii ( $R_S$ ) outside the field of view. For the period before 2300

on day 244, the quality of the transmitted data from the spacecraft was poor, and no useful data are available. Moreover, no continuous emission signals were observed from 1330 to 1700 due to background noise. The lack of a clear signature during these periods precludes a single interpretation. Short-term temporal variability of emission from a Titan-associated cloud is one possibility, although aliasing by the time-dependent background noise seems a more likely explanation. After 1700 on day 245, the field of view moved away from Titan's orbit, and no torus-associated features were observed. The Titan-associated emissions are most likely due to the scattering of the solar hydrogen Ly  $\alpha$  line by an atomic hydrogen cloud along Titan's orbit. These results are consistent with the tentative identification of a cloud by Barker (4), who found a properly Doppler-shifted Ly  $\alpha$  signal while viewing just inside Titan's orbit with an Earth-orbiting ultraviolet spectrometer. The apparent width of the emission signal suggests that the vertical extent of the cloud is about  $1.5 R_S$  (Figs. 2 and 3), and the long duration of the emission signals suggests that the emitted cloud extends at least  $5 R_S$  from Titan's disk. The full extent along the orbit could be much greater, but the present observations would suggest a weaker glow at angular distances greater than the above.

The plasma density at Titan's orbit is estimated to be about  $5 \text{ cm}^{-3}$  or less (5). For corotating plasma (velocity  $V = 200 \text{ km sec}^{-1}$ ) at the radial distance of Titan, the lifetime of local hydrogen atoms against charge exchange is estimated to be about  $10^7$  seconds—quite large compared to the Titan's orbital period ( $4 \times 10^5$  seconds). The lifetime of hydrogen atoms before photoionization is about  $2 \times 10^8$  seconds, which is longer than the lifetime before charge exchange by a factor of 20. Thus Titan's apparent hydrogen cloud would be expected to form a complete torus, and indeed, emission has been detected  $\sim 5 R_S$  from Titan and along its orbit, but the limited amount of data preclude a more definitive statement on the spatial extent of the cloud. Furthermore, the brightness of the observable source has not yet been determined because of a sensitivity change in the  $\lambda_{L1}$  channel during the encounter with the Saturn system.

**Ring emission.** Several Saturn radii outside the A ring, there is a weak glow that may be associated with the ring atomic hydrogen. The glow is brighter near the rings, suggesting that they are a significant source of atomic hydrogen. The glow does not seem uniform in the

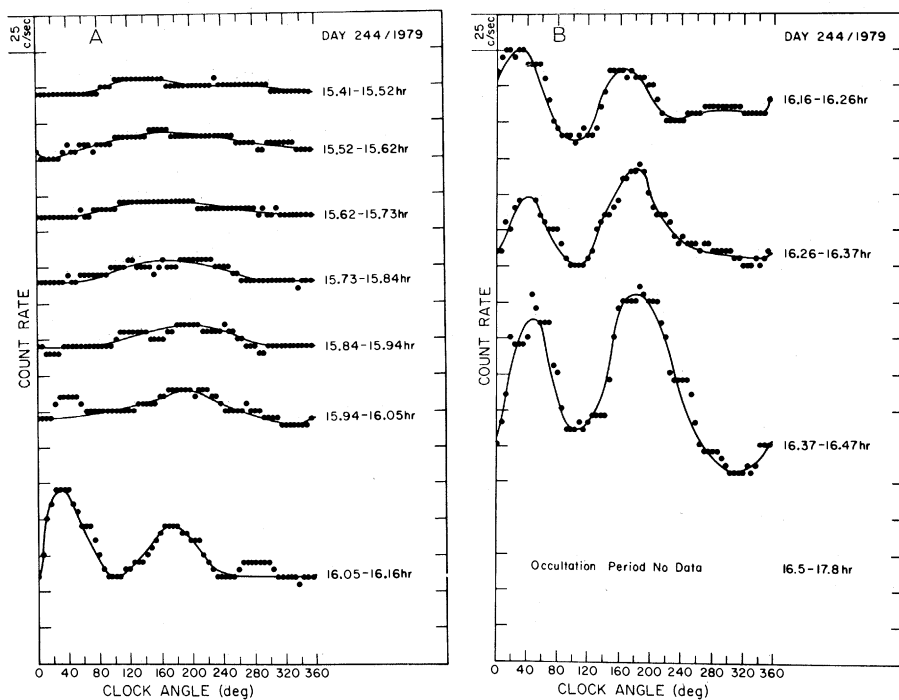


Fig. 4. (A and B) Emission signals from the vicinity of Saturn's rings. The emission features at clock angles  $\sim 40^\circ$  and  $\sim 180^\circ$  are interpreted as resonance scattering of the solar Ly  $\alpha$  line, suggesting a torus of atomic hydrogen.

vicinity of the rings; it is brightest near the B ring. This lack of uniformity suggests that the particles leaving the rings have low kinetic energy, and continue to orbit Saturn at distances not too different from those at which they were formed. Photodissociation of  $H_2O$  has a significant cross section for producing ground-state atomic hydrogen and electronically excited OH (6). Not all absorption processes will result in low-energy hydrogen, however, and this may account for the relatively weak extended glow. In the present discussion we report only the clearly observed B ring observations.

The most obvious emission signals from the vicinity of the ring plane were observed beginning at 1520, when the spacecraft was about 0.65 AU from the inner edge of the B ring. Prior to this, the signal-to-noise ratio was less than 1, the noise being about 4 count/sec in this period. The signal intensity increased as the spacecraft approached the B ring (Fig. 4).

The signals before 1600 were at clock angles from  $120^\circ$  to  $240^\circ$ , where the field of view crosses the inner portion of the ring plane and its vicinity. The observed signals were centered at  $180^\circ$ , suggesting that the region of maximum intensity is about  $0.2 R_S$  under the B ring plane (Fig. 5). However, only the weak background signals were detected at  $\sim 300^\circ$ , where the field of view crosses the outer portion of the A ring plane.

At 1600 and later, the spacecraft flew very close to the B ring and was under its inner edge. Not only did the signal intensity increase significantly, the signals from the B ring were resolved into two sectors, one at a clock angle of  $\sim 40^\circ$  and another at  $\sim 180^\circ$ . These observations are consistent with arguments that the emissions are from the region close to the B ring and with a vertical extent of  $\sim 0.4 R_S$  (Fig. 6).

Strong Ly  $\alpha$  radiation from Saturn's vicinity has been observed from a rocket-borne spectrograph (3). Our measurements confirmed the presence of such radiation and provided spatial resolution not possible in the sounding rocket observations. Moreover, our results show that the most intense emissions probably result from resonance scattering of the solar Ly  $\alpha$  line by atomic hydrogen in the vicinity of the B ring plane. Likely processes for producing atomic hydrogen from the ring material are (i) neutralization of the Saturn photoelectron-ion flux flowing out along magnetic field lines (7) and (ii) photodissociation of the water ice molecules on the surface of the ring materials (8). The presence of the most

intense hydrogen emissions near the B ring may result from an enhanced hydrogen source associated with the relatively high opacity of the B ring.

As mentioned earlier, it has been suggested that the ion flux from Saturn's ionosphere could be neutralized on the ring material and then thermally escape to produce atomic hydrogen in its vicinity (7). However, since the crystal-binding energy of water molecules in the ice mantle is low (9), and since protons and

electrons can react chemically with water molecules (10, 11), the ionospheric particles can remove and dissociate these molecules from the ice mantle. Such a process may be much more important than neutralization followed by thermal escape, but no definitive results are available. Cheng and Lanzerotti (12) have considered the possible "sputtering" effect of the ring particles at the outer edge of the A ring by the trapped energetic protons in Saturn's magnetosphere.

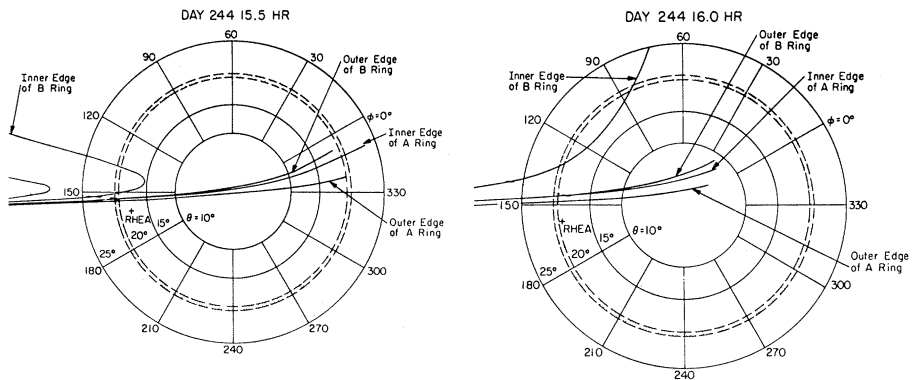


Fig. 5 (left). Viewing geometry for the ultraviolet photometer at 1530 on day 244, as seen along the spin axis of the spacecraft. The field of view ( $\theta = 20^\circ$ ) crosses the ring plane at clock angles  $\sim 150^\circ$  and  $345^\circ$ . Fig. 6 (right). Viewing geometry for the photometer at 1600 on day 244, as seen looking along the spin axis of the spacecraft. The field of view now crosses the inner edge of B ring at clock angles  $\sim 80^\circ$  and  $135^\circ$ . The observed emission features at clock angles  $\sim 40^\circ$  and  $180^\circ$  suggest an extensive hydrogen cloud in the vicinity of the B ring plane.

Fig. 7. Portion of Saturn's disk in the field of view at 1230 on day 244.

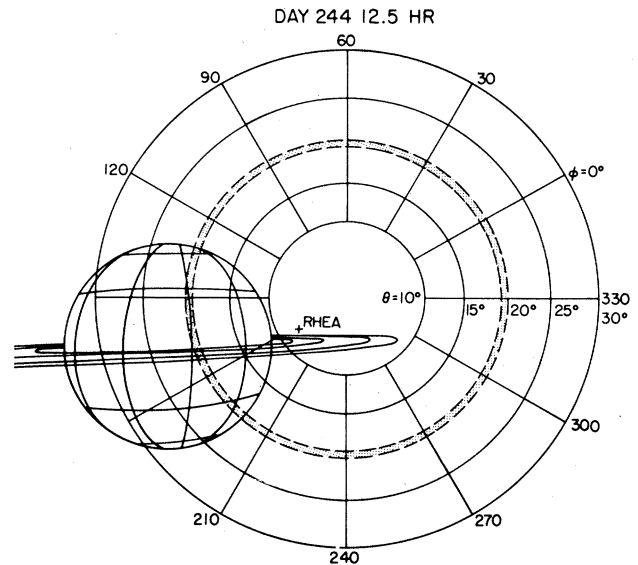
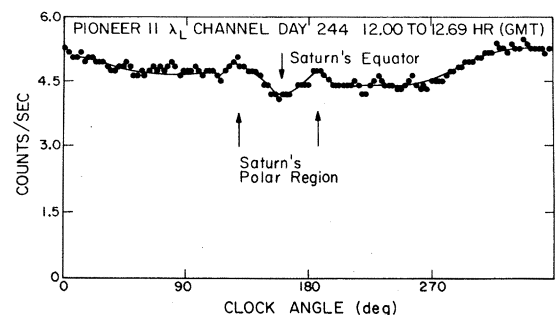


Fig. 8. Emission signals detected in the  $\lambda_L$  channel from Saturn's disk. The enhancement of the emission signal at small and large clock angles corresponds to a slowly changing background signal.



However, such processes should produce a hydrogen cloud with a radius larger than  $2.5 R_S$  and therefore could not account for the observed B ring emission.

*Saturn emission.* The ultraviolet photometer scanned across Saturn's disk during the period from 1000 to 1400 on day 244, when the spacecraft was about  $7.2$  to  $3.5 R_S$  from Saturn. During this period, the equatorial region of Saturn's disk was in the field of view at a clock angle of  $\sim 170^\circ$ , and the whole disk subtended an angle that varied from  $30^\circ$  to  $60^\circ$  (Fig. 7). The observations show Saturn emissions with a strong latitudinal variation superimposed on a slowly varying background (Fig. 8). The emissions around Saturn's polar regions appear stronger than the emission from the equatorial region. This variation could result from limb brightening of Saturn's disk or auroral emission due to particle precipitation in Saturn's atmosphere.

Possible emissions due to helium and perhaps atomic ions have also been detected. However, due to high background noise in our short-wavelength channel, these emissions cannot be positively identified without further data analysis. In addition, photochemical and radiative transfer calculations for Sat-

urn's atmosphere are required to properly interpret the long- and short-wavelength observations.

D. L. JUDGE

F.-M. WU

Department of Physics, University of Southern California, Los Angeles 90007

R. W. CARLSON

Jet Propulsion Laboratory, Pasadena, California 91103

#### References and Notes

1. D. L. Judge and R. W. Carlson, *Science* **183**, 317 (1974).
2. R. W. Carlson and D. L. Judge, *J. Geophys. Res.* **79**, 3623 (1974).
3. H. Weiser, R. C. Vitz, H. W. Moos, *Science* **197**, 755 (1977).
4. E. S. Barker, personal communication.
5. L. A. Frank, personal communication.
6. L. C. Lee, in preparation.
7. W.-H. Ip, *Astron. Astrophys.* **70**, 435 (1978).
8. R. W. Carlson, *Bull. Am. Astron. Soc.* **11**, 557 (1979).
9. N. C. Wickramasinghe, *Interstellar Grains* (Chapman & Hall, London, 1967).
10. \_\_\_\_\_ and D. A. Williams, *Observatory* **88**, 72 (1968).
11. F.-M. Wu, D. L. Judge, R. W. Carlson, *Astrophys. J.* **225**, 325 (1978).
12. A. F. Cheng and L. J. Lanzerotti, *J. Geophys. Res.* **83**, 2597 (1978).
13. We gratefully acknowledge the support that we received throughout this mission from the Pioneer Program Office at NASA headquarters and the Project Office at the NASA/Ames Research Center under the most able direction of C. Hall. We also thank TRW for providing such a reliable spacecraft and Analog Technology Corporation for providing an ultraviolet photometer with the longevity required for a mission to Saturn. Supported by NASA contract NAS 2-6558 with the NASA/Ames Research Center.

3 December 1979

## Imaging Photopolarimeter on Pioneer Saturn

**Abstract.** *An imaging photopolarimeter aboard Pioneer 11, including a 2.5-centimeter telescope, was used for 2 weeks continuously in August and September 1979 for imaging, photometry, and polarimetry observations of Saturn, its rings, and Titan. A new ring of optical depth  $< 2 \times 10^{-3}$  was discovered at 2.33 Saturn radii and is provisionally named the F ring; it is separated from the A ring by the provisionally named Pioneer division. A division between the B and C rings, a gap near the center of the Cassini division, and detail in the A, B, and C rings have been seen; the nomenclature of divisions and gaps is redefined. The width of the Encke gap is  $876 \pm 35$  kilometers. The intensity profile and colors are given for the light transmitted by the rings. A mean particle size  $\leq 15$  meters is indicated; this estimate is model-dependent. The D ring was not seen in any viewing geometry and its existence is doubtful. A satellite, 1979 S 1, was found at  $2.53 \pm 0.01$  Saturn radii; the same object was observed  $\sim 16$  hours later by other experiments on Pioneer 11. The equatorial radius of Saturn is  $60,000 \pm 500$  kilometers, and the ratio of the polar to the equatorial radius is  $0.912 \pm 0.006$ . A sample of polarimetric data is compared with models of the vertical structure of Saturn's atmosphere. The variation of the polarization from the center of the disk to the limb in blue light at  $88^\circ$  phase indicates that the density of cloud particles decreases as a function of altitude with a scale height about one-fourth that of the gas. The pressure level at which an optical depth of 1 is reached in the clouds depends on the single-scattering polarizing properties of the clouds; a value similar to that found for the Jovian clouds yields an optical depth of 1 at about 750 millibars.*

The imaging photopolarimeter (IPP) is a pointable telescope with an aperture of 2.5 cm that utilizes the spin motion of the spacecraft to scan across an object. It may be stepped in a direction per-

pendicular to that of the spacecraft's spin, thus forming a two-dimensional map. There are two wavelength passbands, 390 to 500 nm and 595 to 720 nm. The specifications of the instrument

were published for Pioneer 10 (1) and they are essentially the same for Pioneer 11 (2). A detailed description of the polarimeter has been published (3); the results for Jupiter and interplanetary particles have been overviewed and are referenced in (4). Our Saturn flyby operations have been described (5). Geometric characteristics of our spin-scan imaging data will be discussed in detail elsewhere (6).

After  $6\frac{1}{2}$  years in space, including the active operations during the flyby of Jupiter, the instrument performed remarkably well during the encounter with Saturn. Irregularities in the stepping of the telescope (2) occurred, but nearly all the images can be restored. The aperture wheel, which is the other moving component in this instrument, has functioned almost perfectly. No appreciable degradation has been seen during the Saturn encounter in Channeltron detector sensitivity or in optical transmission; we have not noticed any effects of Saturn's particle radiation.

Our inventory of data is shown in Table 1. The total number of Saturn images ( $0.03^\circ$  aperture) is 440, and 40 of these have a resolution better than the best resolution of ground-based observations (taken as 1200 km); in terms of pixel width, the highest resolution we attained on Saturn was 90 km. For Titan there are five images with a resolution of  $\sim 180$  km.

The Pioneer image converter system (PICS), designed and built at the University of Arizona, was located at Ames Research Center; it allowed the observing team to monitor the imaging data as well as the instrument's operation for subsequent modification of commands to the IPP. The PICS converted the imaging data to color television signals for nationwide programs of the Public Broadcasting System.

Figure 1 shows a full view of the Saturn system. The rings are seen in scattered light; this is different from the view from Earth, where the rings are usually seen in reflected light. During the flyby the sun illuminated the south side of the rings at a small angle ( $\sim 3^\circ$ ) from the ring plane. Pioneer 11 approached from the north on its long transfer trajectory from Jupiter, which had carried it 1.1 AU out of the ecliptic plane, and the planet was observed from the north except between the times of the ring plane crossings ( $\pm 2$  hours from the time of closest approach on 1 September 1979). When seen in scattered light, a ring or a division may be dark because of either large or small optical depth ( $\tau$ ). A bright ring in scattered light implies an intermediate opti-